Membrane Transport, Structure, Function, and Biogenesis:

Inhibitory Regulation of Cystic Fibrosis Transmembrane Conductance Regulator Anion-transporting Activities by Shank2

Joo Young Kim, WonSun Han, Wan Namkung, Ji Hyun Lee, Kyung Hwan Kim, Hyewon Shin, Eunjoon Kim and Min Goo Lee

J. Biol. Chem. 2004, 279:10389-10396.
doi: 10.1074/jbc.M312871200 originally published online December 16, 2003

THE JOURNAL OF BIOLOGICAL CHEMISTRY
Vol. 279, No. 11, Issue of March 12, pp. 10389–10396, 2004

Printed in U.S.A.

Inhibitory Regulation of Cystic Fibrosis Transmembrane Conductance Regulator Anion-transporting Activities by Shank2*

Received for publication, November 25, 2003, and in revised form, December 16, 2003
Published, JBC Papers in Press, December 16, 2003, DOI 10.1074/jbc.M312871200

Joo Young Kim‡, WonSun Han‡, Wan Namkung‡, Ji Hyun Lee‡, Kyung Hwan Kim‡, Hyewon Shin§, Eunjoon Kim§, and Min Goo Lee‡¶

From the ‡Department of Pharmacology and Brain Korea 21 Project for Medical Science, Yonsei University College of Medicine, Seoul 120-752 and the §Creative Research Center for Synaptogenesis and Department of Biological Sciences, Korea Advanced Institute of Science and Technology, Guseong-dong, Daejeon 305-701, Korea

Accumulating evidence suggests that protein-protein interactions play an important role in transepithelial ion transport. In the present study, we report on the biochemical and functional association between cystic fibrosis transmembrane conductance regulator (CFTR) and a PDZ domain-containing protein Shank2. Exploratory reverse transcription-PCR screening revealed mRNAs for several members of PDZ domain-containing proteins in epithelial cells. Shank2, one of these scaffolding proteins, showed a strong interaction with CFTR by yeast two-hybrid assays. Shank2-CFTR interaction was verified by co-immunoprecipitation experiments in mammalian cells. Notably, this interaction was abolished by mutations in the PDZ domain of Shank2. Protein phosphorylation, HCO_3^- transport and Cl^- current by CFTR were measured in NIH 3T3 cells with heterologous expression of Shank2. Of interest, expression of Shank2 suppressed cAMP-induced phosphorylation and activation of CFTR. Importantly, loss of Shank2 by stable transfection of antisense-hShank2 plasmid strongly increased CFTR currents in colonic T84 cells, in which CFTR and Shank2 were natively expressed. Our results indicate that Shank2 negatively regulates CFTR and that this may play a significant role in maintaining epithelial homeostasis under normal and diseased conditions such as those presented by secretory diarrhea.

Secretory epithelia perform vectorial transport of salt and water molecules by coordinated actions of the transporters expressed in polarized epithelial membranes. One of the key membrane proteins regulating overall fluid movements is the cystic fibrosis transmembrane conductance regulator (CFTR),[1] which itself has an anion-transporting activity (1–3). Aberrant membrane transport caused by either hypo- or hyper-functioning of CFTR, can be detrimental, and may result in life-threatening diseases, such as cystic fibrosis or secretory diarrhea (4, 5). Therefore, the fine regulation of salt and water transport is essential in epithelial and body homeostasis.

Accumulating evidence suggests that protein-protein interaction performs an important role in the regulation of transepithelial ion transport (6). Clustering of ion transporters and associated proteins in microdomains of polarized epithelia can facilitate the effective secretion or absorption of salt and water molecules. In this regard, modular adaptor proteins such as PDZ (PSD-95/discs large/ZO-1) domain-containing proteins have drawn increasing attention due to their ability to form supramolecular complexes (7). We have previously shown that the regulatory interaction between CFTR and Na^+/H^+ exchanger 3 (NHE3) through PDZ-based scaffolds is essential for the coordinated regulation of pancreatic bicarbonate secretion (8). In addition, it was found that a number of membrane transporters and receptors participating in pancreatic fluid formation, such as Na^+-HCO_3^- cotransporters (NBC), purinergic receptors, and secretin receptors have a PDZ-binding motif on their C terminus (9, 10). Therefore, multiple protein interactions through PDZ-based scaffolds are believed to perform a critical role in fluid secretion by pancreatic epithelia and possibly by other CFTR-expressing epithelia.

Recently, a large number of PDZ domain-containing proteins were identified in neuronal cells, especially in the postsynaptic density (PSD) of excitatory synapses. Although limited information is available up to now, in general, organization by PDZ-based scaffolds allows the stable localization of interacting proteins and enhances the rate and fidelity of signal transduction (7). Because both neurons and epithelia share many common features, such as ectodermal origin and polarized intracellular structures, it is predicted that some of these scaffolds are expressed in epithelial cells and that they mediate protein-protein interaction. In this study, we aimed to identify the PDZ domain-containing proteins expressed in secretory epithelia and to further characterize their roles in transepithelial ion transport using integrated molecular, biochemical, and physiological approaches.

In an exploratory RT-PCR, it was found that pancreatic epithelia express the mRNAs of several PDZ domain-containing proteins, including SAP97, PSD-95, and Shank2. Of these, Shank2, an isoform of the recently identified family of multimodular adaptors (11), showed an association with CFTR through its PDZ domain in the yeast two-hybrid system and in the mammalian cells. Measurements in CFTR-expressing NIH 3T3 cells revealed that Shank2 overexpression suppressed the cAMP-induced phosphorylation and activation of CFTR. In ad-

* This work was supported by Grant R02-2002-000-00052-0 from the Basic Research Program of the Korea Science & Engineering Foundation and Grant 2001-041-F00110 from the Korea Research Foundation (to M. G. L.), and by the Korean Ministry of Science and Technology (to E. K.). The costs of publication of this article were defrayed in part by the payment of page charges. This article must therefore be hereby marked "*advertisement*" in accordance with 18 U.S.C. Section 1734 solely to indicate this fact.

¶ To whom correspondence should be addressed: Dept. of Pharmacology, Yonsei University College of Medicine, 134 Sinchon-Dong, Seoul 120-752, Korea. Tel.: 82-2-361-5221; Fax: 82-2-313-1894; E-mail: mlee@yumc.yonsei.ac.kr.

[1] The abbreviations used are: CFTR, cystic fibrosis transmembrane conductance regulator; CF, cystic fibrosis; NBC, Na^+-HCO_3^- cotransporter; NHE3, Na^+/H^+ exchanger 3; PDZ, PSD-95/discs large/ZO-1; PSD, postsynaptic density; RT, reverse transcription; aa, amino acid(s); DMEM, Dulbecco's modified Eagle's medium; IP, immunoprecipitation; BCECF-AM, [2′,7′-bis(2-carboxyethyl)-5(6)-carboxyfluorescein]-acetoxymethyl ester; GKAP, guanylate kinase-associated protein.

dition, antisense-Shank2 treatment augmented the CFTR-dependent Cl^- transport in T84 epithelial cells, in which CFTR and Shank2 are endogenously expressed. The above results indicate that Shank2 mediates inhibitory regulation of CFTR and that this may play an important role in epithelial homeostasis.

EXPERIMENTAL PROCEDURES

Materials—The HA-tagged full-length pcDNA3.1-rShank2/CortBP1 construct has been described previously (12). Rabbit polyclonal anti-Shank2 1136 sera were raised against the SAM region of Shank2. To generate H6 fusion proteins for immunization, aa 1012–1252 of rShank2 was amplified by PCR and subcloned into pRSETB (Invitrogen), and fusion proteins were purified using Probond resin (Invitrogen). The specificity of the Shank2 antibody was confirmed by immunoblotting on Shank isoforms expressed in heterologous cells as described previously (13). M3A7 monoclonal antibody against the NBD2 domain and 24-1 monoclonal antibody against the C terminus of CFTR were purchased from Upstate Biotechnologies and R&D systems, respectively. NIH 3T3 cells stably expressing CFTR (1) were kindly provided by Dr. Michael J. Welsh (University of Iowa, Iowa City, IA) and were maintained in Dulbecco's modified Eagle's medium containing 10 mM glucose and 10% fetal calf serum. For the stable expression of Shank2, NIH 3T3 cells were transfected with pcDNA3.1-rShank2 constructs and selected with G418. T84 cells originated from human colonic epithelia were purchased from the American Type Culture Collection (ATCC) and maintained in a 1:1 mixture of Ham's F-12 medium and DMEM supplemented with 5% fetal calf serum.

Yeast Two-hybrid Analysis—The yeast two-hybrid assay was performed as described earlier (14). The L40 yeast strain harboring reporter genes *HIS3* and *LacZ*, under control of the upstream LexA DNA-binding domain, was used in the assay. To semi-quantify the interaction, *HIS3* activity was determined by the percentage of yeast colonies growing on histidine-lacking medium. For pBHA (a bait vector containing the LexA DNA-binding domain) constructs, cDNA sequences containing about 30 aa of the C terminus of membrane proteins were amplified by PCR and subcloned in-frame into pBHA: rNBCn1 (aa 1190–1218: KYSPEKPVSVTINFEDEPSKKYMDA**ETSL**), mDRA (aa 728–757: QEKERKFDFTINTNGGLRNRECQVPV**ETKF**), hCFTR (aa 1452–1480: HRNSSKCKSKPQIAALKEETEEEVQ**DTRL**), hNHE3 (aa 800–831: PFRLSNKSVDSFLQADGPEEQLQPASPE**STHM**), hVIP receptor (aa 467–495: TCSTQVSMLTRVSPGARRSSSFQAE**VSLV**), and rSecretin receptor (aa 421–449: SFSNATNGPTHSTKASTEQSRSIPR**ASII**). The pGAD10 (a prey vector, Clontech) constructs containing the PDZ domains of SAP97, PSD-95, and Shank2 were previously described (12, 14, 15).

RT-PCR—RT-PCR analysis was performed using rat pancreatic tissues and isolated pancreatic duct cells as reported previously (8). The primer sequences used for this study were as follows: 1) rSAP102, sense (GTA CCC GGC AAG AAC ACC CCA AAA CTC AAC), antisense (CCG CAC CAC CAA CCG CAC CAC A), PCR product 432 bp; 2) rSAP97, sense (GTC GTC CTG CCC TCC ACA CCA CA), antisense (CCT TCC GCC TTT TCA CAT ATA ATC GCA CTA), PCR product 376 bp; 3) rGKAP, sense (GAG GCC GTT CAA AGG TCC GTG TGC), antisense (GGG GCC CTT CGC TCC TTC TTG TCA), PCR product 395 bp; 4) rPSD-93, sense (AAG ACT TCC CTG CCG CCC ATC C), antisense (TGC CCC GCC CCC TTC AGT G), PCR product 530 bp; 5) rPSD-95, sense (CCC CAG CCT CCC TTC CCA CCC TTC TTA TTT), antisense (ATG GGG AGT TAT GAT GGG GCA GGG GTG AC), PCR product 373 bp; 6) rShank1, sense (TCT TAT AGG GGG AGC TTT GGA CAC AGG A), antisense (GAC GGG GGA CAG CAG CAT CAC AGG), PCR product 366 bp; 7) rShank2, sense (CCC CGC AGC CGC TCT CCC TCA CT), antisense (CCG CCC TCG CCG ATG CTC AGA ACT T), PCR product 278 bp; 8) rS-SCAM, sense (ACA GGC AGC CAC AGG ATT TTG ATT ATT T), antisense (CAG GCG TGG GGT TCG TCG TGT CTT TAG), PCR product 402 bp.

Immunohistochemistry—The pancreas and colon tissues from Sprague-Dawley rats were embedded in OCT (Miles, Elkhart, IN), frozen in liquid N_2, and cut into 4-μm sections. Immunostaining of frozen sections was performed as previously reported (8). Briefly, the sections were fixed and permeabilized by incubation in cold methanol for 10 min at −20 °C. Nonspecific binding sites were blocked by incubation for 1 h at room temperature with 0.1 ml of phosphate-buffered saline containing 5% goat serum, 1% bovine serum albumin, and 0.1% gelatin (blocking medium). After blocking, the sections were stained by incubating them with anti-Shank2 1136 and/or anti-CFTR 24–1 antibodies and then treated with fluorophore-tagged secondary antibodies. Images were obtained with a Zeiss LSM 510 confocal microscope.

Immunoblotting and Immunoprecipitation—Pre-cleared pancreatic or NIH 3T3 lysates were mixed with the appropriate antibodies and incubated overnight at 4 °C in lysis buffer. Immune complexes were collected by binding to mixed protein A/G beads and were washed four times with lysis buffer prior to electrophoresis. The lysis buffer contains (in mM) HEPES 50 (pH 7.4), NaCl 150, EDTA 1, Nonidet P-40 1% (v/v), glycerol 10% (v/v), and the complete protease inhibitor mixture (Roche Applied Science, Mannheim, Germany). The immunoprecipitates or lysates were suspended in SDS sample buffer and separated by SDS-PAGE. The separated proteins were transferred to polyvinylidene difluoride membranes, and the membranes were blocked by a 1-h incubation at room temperature in a blocking solution containing 5% nonfat dry milk. The membranes were then incubated with the appropriate primary and secondary antibodies, and protein bands were detected by enhanced chemiluminescence solutions (Amersham Biosciences). The staining intensities of immunoblots were analyzed using imaging software (MCID version 3.0; Brock University, St. Catharine's, Ontario, Canada).

Site-directed Mutagenesis—Oligonucleotide-directed mutagenesis was performed using QuikChange kit (Stratagene) with pcDNA3.1-rShank2 plasmid according to the manufacturer's protocol. His-109 residue of rShank2 was substituted with different amino acids. The mutagenesis primers were as follows: H109A, CAA TGA AAA TGT CGT CAA GGT GGG C**GC** **C**AG GCA GGT GGT GAA CAT GAT CCG; H109R, GAA AAT GTC GTC AAG GTG GGC **CGC** AGG CAG GTG GTG AAC ATG ATC; and H109Q, GAA AAT GTC GTC AAG GTG GGC **CAA** AGG CAG GTG GTG AAC ATG ATC. Corresponding antisense primers were also made and used for the PCR reactions to generate plasmids with mutated sequences.

Measurement of Cl^- Channel Activities—Whole cell recordings were performed on CFTR-expressing NIH 3T3 cells after they had been stably transfected with pcDNA3.1-rShank2 or mock plasmids. The pipette solution contained (in mM) 140 *N*-methyl-D-glucamine chloride (NMDG-Cl), 5 EGTA, 1 $MgCl_2$, 1 Tris-ATP, and 10 HEPES (pH 7.2), and the bath solution contained 140 NMDG-Cl, 1 $CaCl_2$, 1 $MgCl_2$, 10 glucose, and 10 HEPES (pH 7.4). All experiments were performed at room temperature (22–25 °C). After establishing the whole cell configuration, CFTR was activated by adding 5 μM forskolin. Currents were digitized and analyzed using an AxoScope 8.1 system and a Digidata 1322A AC/DC converter. Mean currents were normalized as current densities (pA/picofarad (pF)).

Measurement of Cl^-/HCO_3^- Exchange—Cl^-/HCO_3^- exchange activity was measured by recording the intracellular pH (pH_i) in response to $[Cl^-]_o$ changes of the perfusate, as previously detailed (16). Typically, the first 10–40 s of the initial linear portion of pH_i increases due to Cl^--dependent intracellular uptake of HCO_3^- were fitted to a linear equation using the Felix software (version 1.4; PTI Inc.) and expressed as ΔpH units/min. Cell-attached glass coverslips were washed once with HEPES-buffered solution A and assembled to form the bottom of a perfusion chamber. The HEPES-buffered solution A contained (in mM) 140 NaCl, 5 KCl, 1 $MgCl_2$, 1 $CaCl_2$, 10 glucose, and 10 HEPES (pH 7.4). NIH 3T3 cells were loaded with a fluorescent pH probe BCECF by incubating them for 10 min at room temperature in solution A containing 2.5 μM BCECF-AM. After dye loading, the cells were perfused with a HCO_3^--buffered solution and BCECF fluorescence was recorded at excitation wavelengths of 490 and 440 nm at a resolution of 2/s using a recording setup (Delta Ram; PTI Inc.). The HCO_3^--buffered solution containing (in mM) 120 NaCl, 5 KCl, 1 $MgCl_2$, 1 $CaCl_2$, 10 glucose, 5 HEPES, 25 $NaHCO_3$ (pH 7.4) was continuously gassed with 95% O_2 and 5% CO_2. Cl^--free solutions were prepared by replacing Cl^- with gluconate. The 490/440 ratios were calibrated intracellularly by perfusing the cells with solutions containing 145 mM KCl, 10 mM HEPES, and 5 μM nigericin with pH adjusted to 6.2–7.6.

Biotinylation of Surface Membrane Proteins—Surface biotinylation of glycosylated CFTR was performed as described by Lisanti *et al.* (17) with minor modifications. Briefly, cells were washed with ice-cold phosphate-buffered saline containing 0.1 mM $CaCl_2$ and 1 mM $MgCl_2$ and then incubated with 10 mM $NaIO_4$ for 30 min at 0 °C in the dark to increase acceptability of biotin to glycoside moiety. The cells were then washed and biotinylated using EZ-Link biotin-LC-hydrazide (Pierce, 2 mg/ml in solution A) for 30 min at room temperature. Free biotin was washed out twice with a glycine-containing solution (100 mM glycine, 10 mM Tris-HCl, pH 7.4) and then with ice-cold phosphate-buffered saline. For time-course experiments, cells were incubated with DMEM media for 2, 8, 18, or 24 h and lysed with a lysis buffer (1% Triton X-100, 50 mM EGTA, 134 mM NaCl, 10 mM Tris-HCl, pH 7.4, with complete protease

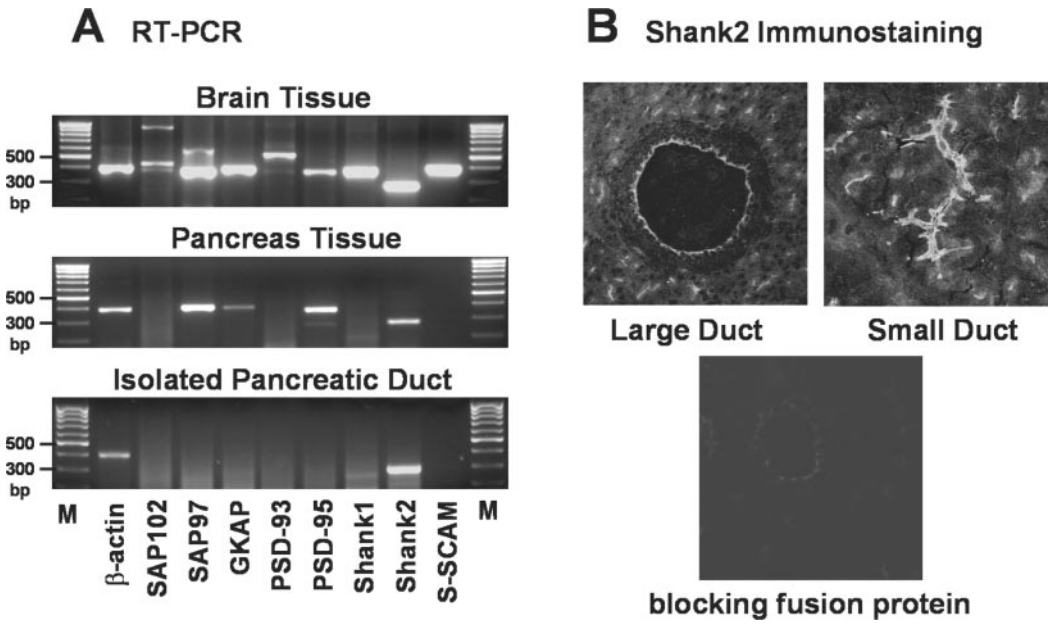

FIG. 1. **Expression of PDZ domain-containing proteins in pancreatic epithelia.** *A*, RT-PCR analyses of PDZ domain-containing proteins identified in the PSD of excitatory synapses were performed on rat pancreatic tissues and on isolated pancreatic ducts. Rat brain tissue samples were used as positive controls. *B*, expression of Shank2 in pancreatic tissues was examined by immunostaining using anti-Shank2 1136 antibody and fluorescein isothiocyanate-labeled goat anti-rabbit IgG sera. Note that Shank2 was localized in the luminal pole of the large (*left*) and the small (*right*) pancreatic duct cells, and that this was absent from the samples incubated with H6-rShank2-(1012–1252) fusion proteins used for immunization (*bottom*). *M*, molecular maker.

inhibitor cocktails). The lysates were centrifuged for 10 min (13,000 × *g*), and the pellet was discarded. Avidin solution (UltraLink Immobilized NeutrAvidin beads 10%, Pierce, 200 μl) was added to the supernatant (500 μg of protein in 500 μl of lysis buffer), and the mixture was incubated overnight with gentle mixing at 4 °C. Avidin-bound complexes were pelleted (13,000 × *g*) and washed three times. Biotinylated proteins were eluted in Laemmli buffer, resolved by SDS-PAGE, electrotransferred, and immunoblotted with the anti-CFTR antibody M3A7.

^{32}P Labeling of CFTR Protein—NIH 3T3 cells grown in 6-well plates were incubated in a phosphate-free DMEM supplemented with 0.5 mCi/ml [^{32}P]orthophosphate (PerkinElmer Life Sciences) for 3 h at 37 °C. The cells were then washed with DMEM and treated with the phosphatase inhibitor $NaVO_4$ (1 mM) and the designated concentrations of forskolin for 10 min. The ^{32}P-labeled lysates (1 mg of protein) were immunoprecipitated with M3A7 CFTR antibody, separated by 6% SDS-PAGE, and visualized by autoradiography.

Antisense mRNA for hShank2 in T84 Cells—Antisense mRNA was expressed in T84 cells to reduce human Shank2 expression. The common 217-bp regions of the two identified splicing variants of hShank2 (NM012309 and NM133266) covering the initiation codon, were selected as target sequences. The target sequences were amplified by PCR and subcloned into pcDNA3.1 vector in the reverse direction using the XhoI and BamHI sites. The primer sequences were as follows: sense (BamHI), CGG GAT CCA TGA TGA TGA ACG TCC CCG; antisense (XhoI), CCG CTC GAG CTG GGA AAG CCG GTG TTG G. Stable transfectants were selected using G418 and the reduced expressions of Shank2 were confirmed by immunoblotting.

Statistical Analysis—Results are presented as the means ± S.E. of the indicated number of experiments. The results of multiple experiments were analyzed using the non-paired Student's *t* test or analysis of variance as appropriate.

RESULTS

Expression of PDZ-based Scaffolds in Pancreatic Epithelia—In previous studies, we reported that interactions between multiple membrane proteins, which have PDZ-binding motif on their C terminus perform important roles in pancreatic bicarbonate secretion (8–10). Therefore, as an initial step, we analyzed the expressions of PDZ domain-containing proteins in pancreatic epithelia by RT-PCR using brain tissue as a positive control. As shown in Fig. 1*A*, rat pancreatic tissue expressed the mRNAs of SAP97, PSD-95, and Shank2. However, pure pancreatic duct cells isolated by microdissection showed only the mRNA of Shank2. Occasionally, a faint band of guanylate kinase-associated protein (GKAP) was observed in samples from pancreatic tissue. The expression of Shank2 in pancreatic tissue was further confirmed by immunostaining (Fig. 1*B*). Of interest, Shank2 was found to be principally localized in the luminal (apical) pole of large and small pancreatic ducts. A weaker expression was also detected in the luminal area of pancreatic acinar cells (Fig. 1*B*).

TABLE I
Yeast two-hybrid assay

HIS3 activity was determined by the percentage of yeast colonies growing on histidine-lacking medium to estimate the intensity of protein-protein interactions between the PDZ domains of adaptor proteins and the C terminus of membrane proteins. After the transfection with the prey and bait vectors, equal amounts of yeast cells were plated on histidine-lacking and histidine-supplemented media. The number of yeast colonies growing on histidine-lacking medium was divided by that of growing on histidine-supplemented medium and expressed as percentage.

Membrane protein	*HIS3* activity			
	pGAD10, alone[a]	SAP97, PDZ1–2	PSD-95, PDZ1–3	Shank2, PDZ
	%			
CFTR	0	0	0	33
NHE3	0	0	0	44
NBCn1	0	1	2	44
DRA	0	0	0	0
VIP receptor	0	1	11	0
Secretin receptor	0	0	0	0

[a] Empty pGAD10 was used as negative control.

Protein-Protein Interaction between PDZ-based Scaffolds and Membrane Proteins—Possible interactions between the C termini of membrane proteins in pancreatic epithelia and the PDZ domains of SAP97, PSD-95, and Shank2 were screened by the yeast two-hybrid assay. Peptide sequences of class I PDZ-binding motif of the membrane proteins are listed under "Experimental Procedures." To estimate the intensity of the protein interactions, *HIS3* activity was determined by the percentage of yeast colonies growing on histidine-lacking

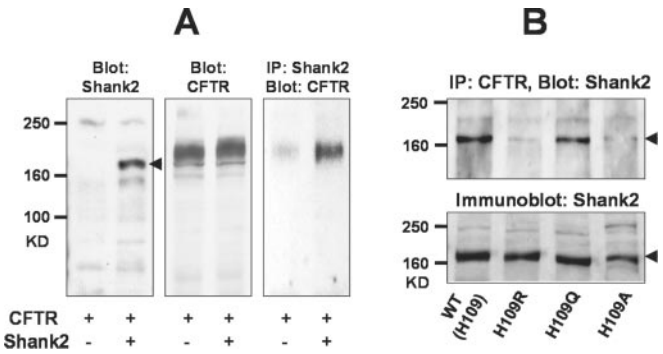

FIG. 2. **Immunoprecipitation of Shank2 and CFTR in NIH 3T3 cells.** *A*, proteins from CFTR-expressing NIH 3T3 cells stably transfected with pcDNA3.1-rShank2/CortBP1 or mock plasmids were precipitated with anti-Shank2 1136 antibody, and then blotted with the anti-CFTR M3A7 antibody. A blot of immunoprecipitated samples is shown in the *right panel* and control immunoblots of Shank2 and CFTR are presented in the *left* and *middle panels*, respectively. *B*, His-109 of rShank2 (position αB1 in the class I PDZ domain) was substituted with Arg, Gln, and Ala, and Shank2-CFTR binding was measured by immunoprecipitation (IP). Note that IP in *panel B* was performed using a different antibody order from that in *panel A*. In all immunoblotting experiments, 100 μg of protein was loaded into each lane, and IP was performed using a total of 1 mg of lysate.

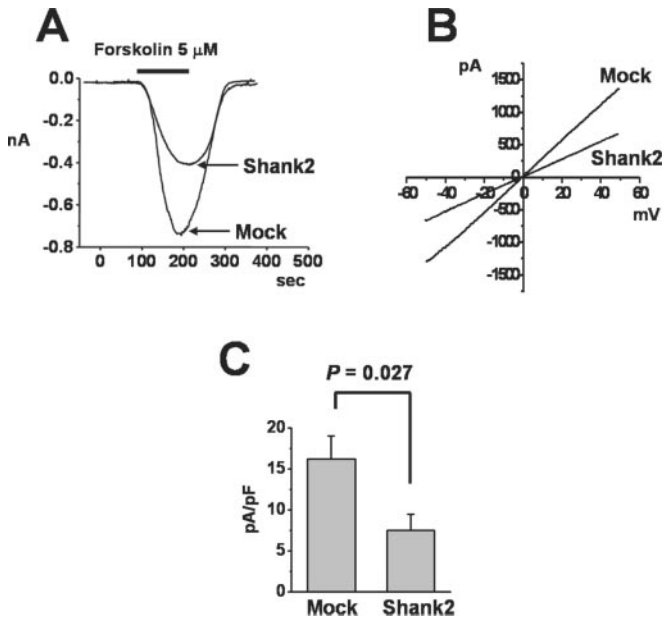

FIG. 3. **Inhibition of CFTR Cl^- channel activity by Shank2 in NIH 3T3 cells.** Cl^- channel activities were measured in CFTR-expressing NIH 3T3 cells stably transfected with pcDNA3.1-rShank2/CortBP1 or mock plasmids in the whole cell configuration. *A*, forskolin treatment produced an inward current in the NMDG-Cl solutions at a holding potential of −30 mV. *B*, linear I-V relationships were observed when a ramp pulse from −50 mV to +50 mV was applied at peak current. *C*, peak currents were normalized as current densities (pA/pF) and the results of 8 (*Mock*) and 10 (*Shank2*) experiments are summarized in *panel C*.

(His^-) medium with empty pGAD10 as negative controls. Positive colonies (His^- growth) were confirmed twice by the β-galactosidase activity. In the yeast two-hybrid screening, Shank2 showed a strong association with CFTR, NHE3, and NBCn1 (Table I). Among the possible Shank2-associated membrane transporters, we chose CFTR for further studies, because CFTR is known to perform a central role in luminal ion transport and to have regulatory functions on the other two transporters, NHE3 and NBCn1 (8, 10). To verify the interaction between CFTR and Shank2 in mammalian cells, CFTR-expressing NIH 3T3 cells were stably transfected with pcDNA3.1-rShank2 or with mock plasmids, and immunoprecipitation (IP) experiments were performed. As shown in Fig. 2*A*, transfection of pcDNA3.1-rShank2 induced expression of Shank2 protein in NIH 3T3 cells (*arrowhead*). Notably, large amounts of CFTR proteins were detected in anti-Shank2 IP samples from Shank2-transfected cells (Fig. 2*A*, *right*). Co-IP experiments using antibodies in reverse order also demonstrated the association between Shank2 and CFTR (see Fig. 2*B*).

It has been reported that the first histidine residue of the second α-helix of PDZ domain (position αB1, His-109 in rShank2) plays an important role in class I PDZ interaction by forming a strong hydrogen bond between its N-3 nitrogen and the hydroxyl group of the −2 serine/threonine residue of the ligand (18). To verify the importance of the PDZ-domain in CFTR-Shank2 interaction, we substituted His-109 with two other amino acids containing nitrogen side chain (H109R and H109Q) and with a hydrophobic amino acid (H109A) and then measured the protein-protein interaction by IP. As shown in Fig. 2*B*, CFTR-Shank2 interactions were abolished in H109R and H109A mutants by 78 ± 8% and 96 ± 3%, respectively (n = 4). Therefore, it was concluded that PDZ-based interactions are required for CFTR-Shank2 binding.

Inhibition of CFTR-dependent Anion Transport by Shank—It is well known that CFTR protein has a cAMP-activated Cl^- channel function (1). Thus, the cAMP-activated chloride channel activities of CFTR-expressing NIH 3T3 cells were measured in the whole cell configuration after they had been stably transfected with pcDNA3.1-rShank2 or mock plasmids. Treatment with the adenylyl cyclase activator forskolin produced a large inward current in NMDG-Cl solutions with linear I-V relationships (Figs. 3, *A* and *B*). Further treatment with 5-nitro-2-(3′-phenylpropylamino)benzoic acid (30 μM) inhibited this current by 94 ± 3% (not shown). These characteristics were in line with previous observations of CFTR Cl^- currents (2). Interestingly, Shank2 overexpression decreased the CFTR current densities (pA/pF) by 53% (Fig. 3*C*).

Recently, it was found that CFTR plays an important role in transepithelial HCO_3^- transport by regulating Cl^-/HCO_3^- exchange (2, 19). Moreover, reduced HCO_3^- secretion by defective CFTR-dependent HCO_3^- transport has been suggested to be an important pathological mechanism in mutant CFTR-induced respiratory and pancreatic diseases (21, 22). Therefore, Cl^-/HCO_3^- exchange activities were measured in NIH 3T3 cells by estimating the pH_i increase due to Cl^- removal from HCO_3^--buffered perfusate. As reported earlier (2), the Cl^-/HCO_3^- exchange activities of CFTR-expressing NIH 3T3 cells were highly increased by forskolin stimulation (Fig. 4*B*), but those of CFTR-non expressing cells were unchanged (Fig. 4*A*). The basal and forskolin-stimulated activities of CFTR-expressing NIH 3T3 cells were 0.121 ± 0.026 ΔpH unit/min and 0.865 ± 0.150, respectively. In Shank2-overexpressing cells, basal activity (0.079 ± 0.018, p = 0.22) was not significantly changed compared with mock transfected cells. However, similar to the results of whole cell Cl^- currents, Shank2 overexpression decreased the cAMP-activated Cl^-/HCO_3^- exchange (0.398 ± 0.093, p = 0.02) in CFTR-expressing NIH 3T3 cells (Fig. 4*D*).

Molecular Mechanisms Responsible for the Decreased CFTR Activity—Two possibilities were examined to explain the underlying molecular mechanisms of inhibitory effects of Shank2 on CFTR-dependent anion transporting activities. The first possibility involves the reduced membrane expression of CFTR protein. Because Shank2 is known to be associated with cytoskeletal proteins (11), it may affect sorting, trafficking, or the endocytotic recycling of CFTR protein. Membrane proteins were biotinylated and harvested at the designated times and

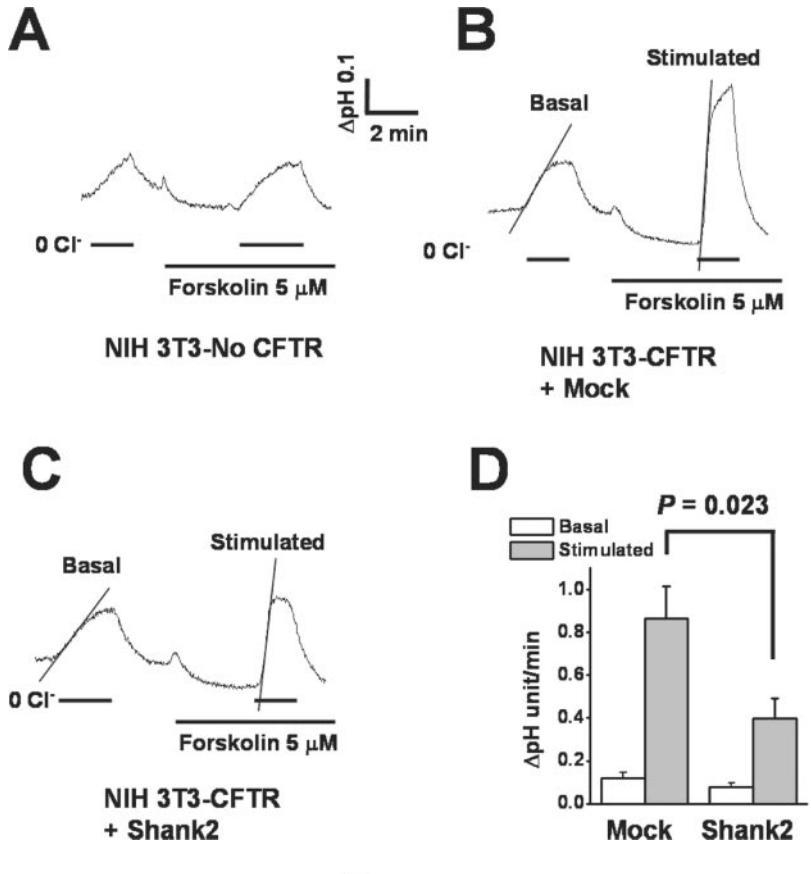

FIG. 4. **Inhibition of CFTR-dependent Cl^-/HCO_3^- exchange by Shank2 in NIH 3T3 cells.** CFTR-dependent Cl^-/HCO_3^- exchanges were analyzed in NIH 3T3 cells by measuring the increase in intracellular pH (pH_i) in response to $[Cl^-]_o$ removal from the HCO_3^--containing perfusate (25 mM HCO_3^-, continuously gassed with 95% O_2 and 5% CO_2). The Cl^-/HCO_3^- exchange activities of CFTR-expressing NIH 3T3 cells were markedly increased by forskolin stimulation (*B*), but those of CFTR-non expressing cells were unchanged (*A*). Shank2 overexpression reduced forskolin-stimulated Cl^-/HCO_3^- exchange (*B–D*).

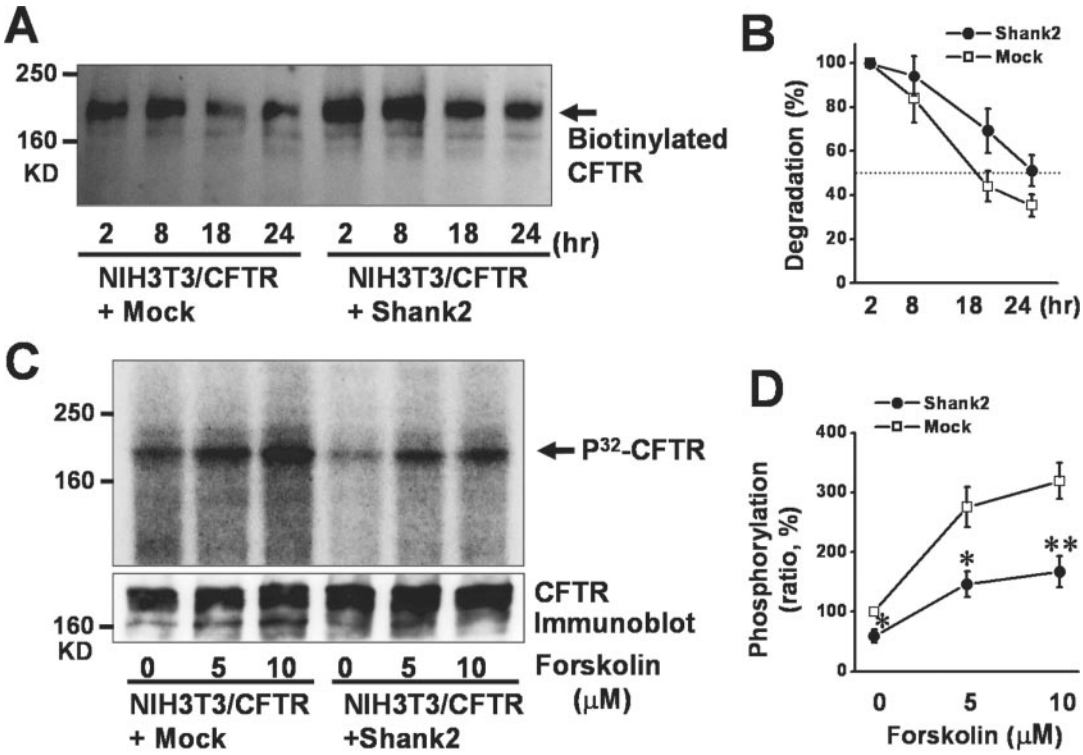

FIG. 5. **Surface biotinylation and phosphorylation of CFTR in NIH 3T3 cells.** *A* and *B*, membrane proteins were biotinylated for 30 min and harvested at pre-set times. Biotinylated proteins were resolved by SDS-PAGE and immunoblotted with the anti-CFTR M3A7 antibody. Degradation of surface CFTR protein in pcDNA3.1-rShank2 or mock-transfected cells was estimated treating each band intensity at 2 h as 100%. Results of three experiments are summarized in *panel B*. *C* and *D*, ^{32}P labeling of CFTR protein was performed in NIH 3T3 cells stimulated with forskolin. Individual phosphorylation levels were compared with the basal level (0 μM forskolin) in mock transfected cells, and the results of four experiments are summarized in *panel D*. *, $p < 0.05$; **, $p < 0.01$; difference from mock.

then blotted with anti-CFTR M3A7 antibody (Fig. 5*A*). In contrast to our expectations, Shank2 overexpression showed a tendency to increase the membrane expression of CFTR by 39 ± 28% ($p = 0.11$, at 2 h after biotinylation) and to extend the half-life of the biotinylated CFTR protein from 17.2 to 25.4 h ($p = 0.13$, Fig. 5*B*), although neither of them reached the statistical

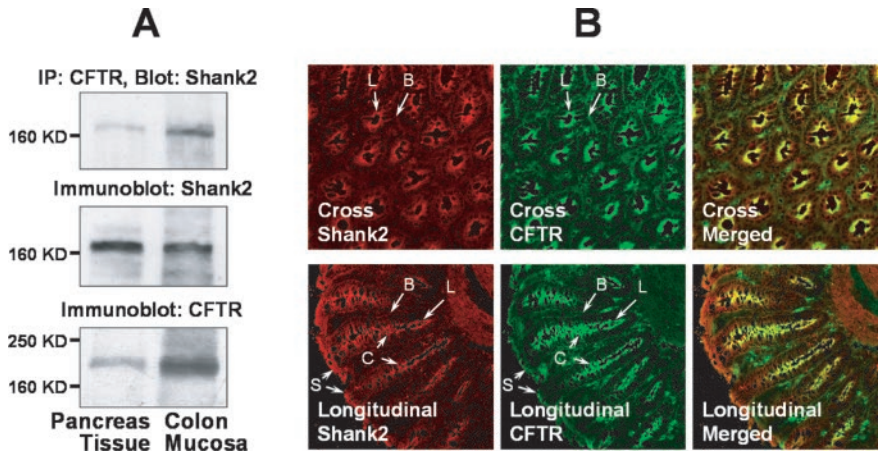

FIG. 6. **Expression of Shank2 in rat colonic mucosa.** *A*, expressions of CFTR (*bottom*) and Shank2 (*middle*) were compared in rat pancreatic tissue and colonic mucosa by immunoblotting (each 100 μg of protein). In the immunoprecipitation experiment (*upper*), samples from colonic mucosa showed a 3.1 times thicker band intensity than those from the pancreas tissue (each performed with 2 mg of protein). *B*, immunostaining for Shank2 in colonic mucosa was performed using anti-Shank2 1136 (*red*) and anti-CFTR 24–1 (*green*) antibodies. *S*, surface cells; *C*, crypt cells; *B*, basolateral membrane; *L*, luminal membrane.

significance. Nonetheless, the results of biotinylation experiments did not explain the reduced CFTR activity by Shank2.

The second possibility of the reduced CFTR activity would be the decreased cAMP-induced phosphorylation of CFTR upon Shank2 expression. It is widely accepted that cAMP/PKA-induced phosphorylation performs critical roles in CFTR activation (23). To measure the levels of phosphorylation, ^{32}P labeling of CFTR protein was performed in NIH 3T3 cells (nominally *in vivo* phosphorylation assay) by stimulating with forskolin and treating with the phosphatase inhibitor $NaVO_4$ (Fig. 5*C*). A control CFTR immunoblotting was performed to verify that similar amounts of CFTR protein were loaded in each lane (Fig. 5*C*, *bottom panel*). In each experiment, the phosphorylation levels of individual lanes were compared with the basal level (0 μM forskolin) in mock transfected cells, and the summarized results of four experiments are illustrated in Fig. 5*D*. Of note, Shank2 overexpression decreased the cAMP-induced phosphorylation of CFTR as well as the basal phosphorylation. Hence, it was concluded that the down-regulation of CFTR activity by Shank2 was possibly due to the reduced cAMP-induced phosphorylation of CFTR.

CFTR-Shank2 Interaction in Colonic Epithelia—Either hyper- or hypofunction of CFTR perturbs the epithelial homeostasis (4, 5). Concerning the inhibitory regulation of Shank2 on CFTR, colonic epithelia will be the most relevant tissue to examine the physiological role of Shank2, where hyper-functioning of CFTR causes severe life-threatening conditions such as cholera (5, 24). Initially, we investigated the expression of Shank2 in rat colonic mucosa. As shown in Fig. 6*A*, Shank2 was expressed in colonic mucosa, in fact, higher amounts of CFTR-Shank2 IP products were observed in samples from colonic mucosa than in those from the pancreatic tissue, possibly due to the higher amount of CFTR protein in the colonic mucosa. The expression pattern of Shank2 was determined immunohistochemically by double staining with anti-Shank2 and anti-CFTR antibodies (Fig. 6*B*). In general, colonic surface epithelia absorb fluids and electrolytes, whereas crypt cells secrete (5). Shank2 was expressed in both surface and crypt cells, although CFTR was expressed principally in crypt cells. As was found in pancreatic epithelia (Fig. 1*B*), Shank2 was observed in the luminal area of colonic epithelia. Therefore, merged images in cross sections and in longitudinal sections showed that Shank2 and CFTR were highly co-localized in the luminal area of crypt cells (Fig. 6*B*).

To determine whether the Shank2-mediated inhibition of CFTR has physiological relevance, we attempted to remove Shank2 from colonic T84 cells by stably transfecting antisense-hShank2 clones. As shown in Fig. 7*A*, antisense-Shank2 treatment caused an average reduction of 79 ± 8% in Shank2

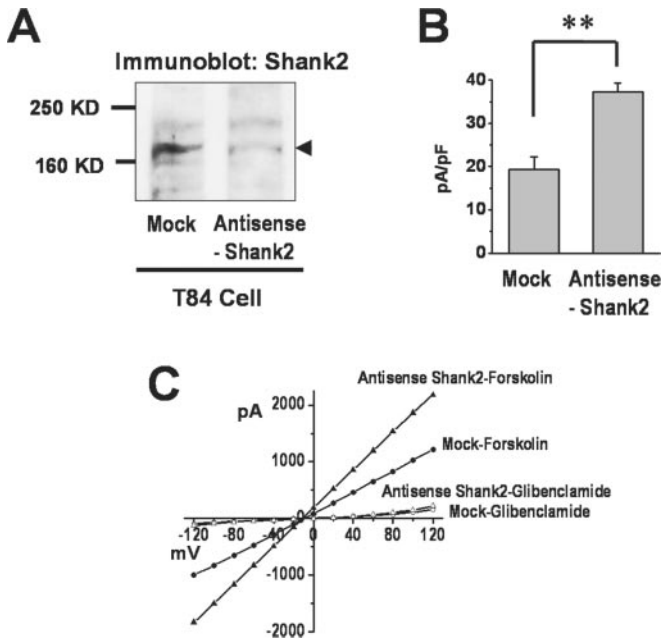

FIG. 7. **Measurement of CFTR activity in antisense-hShank2 treated T84 cells.** *A*, the stable transfection of antisense-hShank2 reduced Shank2 protein expression by 79 ± 8% in T84 cells (n = 3). *B*, summarized results of whole cell Cl^- channel recordings in T84 cells taken at a holding potential of −40 mV. Cells were stimulated with forskolin (5 μM), and peak currents were normalized as current densities. *C*, representative traces of I-V relationships (step pulse from −120 mV to +120 mV with 20-mV intervals) obtained from cells having median value of each group. **, $p < 0.01$; difference from mock.

protein expression in T84 cells. We next examined the effects of Shank2 loss on CFTR activity by whole cell patch-clamp studies. A summary of the Cl^- current recordings taken at a holding potential of −40 mV is presented in Fig. 7*B*. Interestingly, only a proportion of T84 cells showed significant CFTR Cl^- channel activities. We regarded the cells showed the forskolin-stimulated current densities over 5 pA/pF as "CFTR-positive," and analyzed their values for evaluating the effects of Shank2 expression. The proportion of CFTR-positive cells was not different between the mock and the antisense-Shank2-treated cells (7/24 and 5/14, respectively; p = 0.72 by Fisher's exact test). In all experiments, the viability of cells was verified by observing volume-sensitive Cl^- channel activities evoked by 260 mosM bath solutions after the forskolin treatment. Notably, loss of Shank2 by antisense treatment augmented CFTR currents in T84 cells, in which Shank2 and CFTR are endogenously expressed. Forskolin (5 μM) produced an average in-

ward current of −19.3 ± 2.9 pA/pF at a −40 mV holding potential in mock transfected cells, and this value was increased to −37.3 ± 3.7 pA/pF ($p < 0.01$) in antisense-hShank2-transfected cells (Fig. 7*B*). Traces of I-V relationships obtained from cells having median value of each group are shown in Fig. 7*C*. Forskolin treatment evoked an inward current in NMDG-Cl solutions with linear I-V relationships. In addition, an average inhibition of 91% of this current by glibenclamide (100 μM) demonstrated that most of the observed currents were induced by CFTR.

DISCUSSION

Assembly of specific proteins at the microdomains of intracellular regions is powerful machinery that enables the cell to function properly as well as to form unique subcellular structures. One of the critical components of these protein complexes is the modular adaptor proteins. Recently, a family of PDZ-based adaptors has been identified by several investigators and named independently as Shank, CortBP, or ProSAP (11, 25, 26). Subsequent studies revealed that the Shank family of proteins has many binding partners especially in the PSD of excitatory synapses (12). For example, Shank interacts directly with GKAP and Homer, thus potentially bridging the NMDA receptor and the metabotropic glutamate receptors in neurons (27). However, the results of present study demonstrate that the role of Shank as a molecular scaffold is not limited to the neuronal systems.

The most notable finding in this study is the inhibition of CFTR activity by Shank2. CFTR-dependent Cl^- channel activities and Cl^-/HCO_3^- exchange activities were decreased by Shank2 overexpression in CFTR-expressing NIH 3T3 cells (Figs. 3 and 4). In addition, cAMP-induced phosphorylation of CFTR was decreased by Shank2 in the heterologous expression system (Fig. 5, *C* and *D*). Importantly, loss of Shank2 by antisense-Shank2 treatment increased CFTR-mediated Cl^- channel activities in colonic T84 cells, in which epithelial properties were retained (Fig. 7). All the above findings suggest that Shank2 has a tonic inhibitory effect on the anion-transporting activities of CFTR. Considering the fact that uncontrolled hyperactivation of CFTR evokes life-threatening secretory diarrhea, Shank2 may play a significant role in the homeostatic regulation of CFTR activity at least in colonic epithelia.

As to the experiments in T84 cells, we found that there are considerable degrees of heterogeneity of CFTR activity between batches. In fact, we measured the CFTR Cl^- channel activity in T84 cells from three different sources. Among them, a batch obtained directly from ATCC (CCL-248, lot number 2056314) showed the highest CFTR activity in terms of both the frequency of CFTR-positive cells and the amplitude of CFTR Cl^- currents. Therefore, stable transfection of antisense-Shank2 plasmid was introduced to this batch of T84 cells and functional experiments were performed. However, low expression of CFTR protein in T84 cells hampered the further molecular analyses that had been conducted in NIH 3T3 cells. Although the results in heterologous expression system do not always match with native expression system, we speculate that significant analogy exists between these two systems, because expression of Shank2 inhibited CFTR activity in both NIH 3T3 and T84 cells.

The finding that a protein can bind to CFTR and inhibit its activity is reminiscent of the relationship between syntaxin 1A and CFTR (28). However, in several respects, the inhibitory mechanism of Shank2 on CFTR is different from that of syntaxin 1A. For example, syntaxin 1A binds to the N-terminal part of CFTR and is believed to regulate CFTR activity by directly modulating the gating properties or by affecting membrane trafficking of CFTR (29). On the contrary, Shank2 seems to bind to the C-terminal PDZ-binding motif of CFTR (Table I and Fig. 2*B*) and regulate its anion transporting activities by inhibiting cAMP-induced phosphorylation (Fig. 5). The mechanisms responsible for the reduced cAMP-induced phosphorylation are currently under investigation. A plausible scenario is that Shank2 associates with a phosphatase that can dephosphorylate CFTR. Alternative possibilities include the competition between Shank2 and CFTR-activating scaffolds at the C terminus of CFTR. For example, PDZ-based scaffolds, such as EBP50/NHERF1, E3KARP/NHERF2, or PDZK1/CAP70 have been suggested to activate CFTR by facilitating protein kinase A-induced phosphorylation or by forming active dimer (30–32). Although the present study sufficiently showed that Shank2 decreased CFTR phosphorylation (Fig. 5), this does not completely rule out other possible mechanisms for the reduced CFTR activity. For instance, Shank2 has a single PDZ domain, hence it can hamper the reported active dimer formation by multiple PDZ domain-containing scaffolds (32). The competitive balance between Shank2-CFTR binding and EBP50-CFTR binding (or E3KARP-CFTR or CAP70-CFTR) may maintain the homeostatic regulation of CFTR.

By the yeast two-hybrid screening, it was found that Shank2 can associate with NHE3 and NBCn1 in addition to CFTR. Notably, all of these transporters are localized in the luminal membrane of pancreatic duct cells and actively participate in transepithelial HCO_3^- transport (8, 10). In fact, we observed that Shank2 binds to NHE3, and that the overexpression of Shank2 blunted the cAMP-induced inhibition of NHE3 activity in the heterologous expression system of PS120 cells (not shown). These findings imply that Shank2 works as a common regulator for modulating ion and fluid transport in the luminal membrane of epithelia, especially as a counterpart of cAMP-evoked signals. Typically, the Shank family of proteins has multiple protein-protein interaction sites and is characterized by multiple ankyrin repeats, an SH3 domain, a PDZ domain, a long proline-rich domain, and a sterile alpha motif (SAM) domain in N terminus to C terminus order. However, isoforms and splicing variants of Shank showed a considerable degree of variability in their domain compositions (11, 13). Although the name of Shank originated from SH3 domain and ankyrin repeats, the major form of Shank2/CortBP1 found and used in this study does not have SH3 or ankyrin repeat domains, but does have the other three domains, including the PDZ domain. Future studies identifying binding partners for these modular domains may reveal more diverse roles of Shank2 proteins in epithelial function.

In conclusion, we found that Shank2 binds to CFTR and tonically inhibits the cAMP-induced activation of CFTR after an integrated search for new PDZ-based scaffolds in epithelial tissues. Because aberrant CFTR activity, especially uncontrolled hyper-functioning of CFTR evokes life-threatening conditions such as diarrhea in cholera infection, the fine regulation of CFTR activity by Shank2 will be important in maintaining epithelial and body homeostasis.

REFERENCES

1. Anderson, M. P., Rich, D. P., Gregory, R. J., Smith, A. E., and Welsh, M. J. (1991) *Science* **251,** 679–682
2. Lee, M. G., Wigley, W. C., Zeng, W., Noel, L. E., Marino, C. R., Thomas, P. J., and Muallem, S. (1999) *J. Biol. Chem.* **274,** 3414–3421
3. Schwiebert, E. M., Benos, D. J., Egan, M. E., Stutts, M. J., and Guggino, W. B. (1999) *Physiol. Rev.* **79,** S145–S166
4. Quinton, P. M. (1999) *Physiol. Rev.* **79,** S3–S22
5. Kunzelmann, K., and Mall, M. (2002) *Physiol. Rev.* **82,** 245–289
6. Kunzelmann K. (2001) *News Physiol. Sci.* **16,** 167–170
7. Sheng, M., and Sala C. (2001) *Annu. Rev. Neurosci.* **24,** 1–29
8. Ahn, W., Kim, K. H., Lee, J. A., Kim, J. Y., Choi, J. Y., Moe, O. W., Milgram, S. L., Muallem, S., and Lee, M. G. (2001) *J. Biol. Chem.* **276,** 17236–17243
9. Lee, M. G., Ahn, W., Lee, J. A., Kim, J. Y., Choi, J. Y., Moe, O. W., Milgram, S. L., Muallem, S., and Kim, K. H. (2001) *J. Pancreas* **2,** Suppl. 4, 203–206
10. Park, M., Ko, S. B., Choi, J. Y., Muallem, G., Thomas, P. J., Pushkin, A., Lee,

M. S., Kim, J. Y., Lee, M. G., Muallem, S., and Kurtz, I. (2002) *J. Biol. Chem.* **277,** 50503–50509
11. Sheng, M., and Kim, E. (2000) *J. Cell Sci.* **113,** 1851–1856
12. Park, E., Na, M., Choi, J., Kim, S., Lee, J. R., Yoon, J., Park, D., Sheng, M., and Kim, E. (2003) *J. Biol. Chem.* **278,** 19220–19229
13. Lim, S., Naisbitt, S., Yoon, J., Hwang, J. I., Suh, P. G., Sheng, M., and Kim, E. (1999) *J. Biol. Chem.* **274,** 29510–29518
14. Kim, E., Niethammer, M., Rothschild, A., Jan, Y. N., and Sheng, M. (1995) *Nature* **378,** 85–88
15. Mok, H., Shin, H., Kim, S., Lee, J. R., Yoon, J., and Kim, E. (2002) *J. Neurosci.* **22,** 5253–5258
16. Namkung, W., Lee, J. A., Ahn, W., Han, W., Kwon, S. W., Ahn, D. S., Kim, K. H., and Lee, M. G. (2003) *J. Biol. Chem.* **278,** 200–207
17. Lisanti, M. P., Le Bivic, A., Sargiacomo, M., and Rodriguez-Boulan, E. (1989) *J. Cell Biol.* **109,** 2117–2127
18. Doyle, D. A., Lee, A., Lewis, J., Kim, E., Sheng, M., and MacKinnon, R. (1996) *Cell* **85,** 1067–1076
19. Lee, M. G., Choi, J. Y., Luo, X., Strickland, E., Thomas, P. J., and Muallem, S. (1999) *J. Biol. Chem.* **274,** 14670–14677
20. Ko, S. B. H., Shcheynikov, N., Choi, J. Y., Luo, X., Ishibashi, K., Thomas, P. J., Kim, J. Y., Kim, K. H., Lee, M. G., Naruse, S., and Muallem, S. (2002) *EMBO J.* **21,** 5662–5672
21. Choi, J. Y., Muallem, D., Kiselyov, K., Lee, M. G., Thomas, P. J., and Muallem, S. (2001) *Nature* **410,** 94–97
22. Quinton, P. M. (2001) *Nat. Med.* **7,** 292–293
23. Dahan, D., Evagelidis, A., Hanrahan, J. W., Hinkson, D. A., Jia, Y., Luo, J., and Zhu, T. (2001) *Pflugers Arch.* **443,** Suppl. 1, S92–S96
24. Gabriel, S. E., Brigman, K. N., Koller, B. H., Boucher, R. C., and Stutts, M. J. (1994) *Science* **266,** 107–109
25. Naisbitt, S., Kim, E., Tu, J. C., Xiao, B., Sala, C., Valtschanoff, J., Weinberg, R. J., Worley, P. F., and Sheng, M. (1999) *Neuron* **23,** 569–582
26. Boeckers, T. M., Bockmann, J., Kreutz, M. R., and Gundelfinger, E. D. (2002) *J. Neurochem.* **81,** 903–910
27. Tu, J. C., Xiao, B., Naisbitt, S., Yuan, J. P., Petralia, R. S., Brakeman, P., Doan, A., Aakalu, V. K., Lanahan, A. A., Sheng, M., and Worley, P. F. (1999) *Neuron* **23,** 583–592
28. Naren, A. P., Nelson, D. J., Xie, W., Jovov, B., Pevsner, J., Bennett, M. K., Benos, D. J., Quick, M. W., and Kirk, K. L. (1997) *Nature* **390,** 302–305
29. Cormet-Boyaka, E., Di, A., Chang, S. Y., Naren, A. P., Tousson, A., Nelson, D. J., and Kirk, K. L. (2002) *Proc. Natl. Acad. Sci. U. S. A.* **99,** 12477–12482
30. Short, D. B., Trotter, K. W., Reczek, D., Kreda, S. M., Bretscher, A., Boucher, R. C., Stutts, M. J., and Milgram, S. L. (1998) *J. Biol. Chem.* **273,** 19797–19801
31. Sun, F., Hug, M. J., Lewarchik, C. M., Yun, C. H., Bradbury, N. A., and Frizzell, R. A. (2000) *J. Biol. Chem.* **275,** 29539–29546
32. Wang, S., Yue, H., Derin, R. B., Guggino, W. B., and Li, M. (2000) *Cell* **103,** 169–179